Crystal Structure, Electronic Structure, and Temperature-Dependent Raman Spectra of $Tl[Ag(CN)_2]$: Evidence for Ligand-Unsupported Argentophilic Interactions

Mohammad A. Omary,[†] Thomas R. Webb,[‡] Zerihun Assefa,[§] George E. Shankle,[||] and Howard H. Patterson*[,†]

Department of Chemistry, University of Maine, Orono, Maine 04469, Department of Chemistry, Auburn University, Auburn, Alabama 36849, Oak Ridge National Laboratory, P.O. Box 2008, Oak Ridge, Tennessee 37831, and Angelo State University, San Angelo, Texas 76909

Received June 5, 1997

The structure of thallium dicyanoargentate(I) has been determined crystallographically. The crystal structure shows an Ag−Ag distance of 3.11 Å. This is the shortest Ag−Ag distance reported for any silver dicyanide salt whose crystal structure has been determined. Raman spectra of the compound show four ν_{C-N} peaks that are well-resolved in the 10−80 K temperature range. This result agrees well with group theory analysis. Extended Hückel calculations using relativistic wave functions have been carried out for two models which describe the interactions between the $Ag(CN)_2^-$ ions within the crystal structure of $Tl[Ag(CN)_2]$. The results of these calculations indicate the formation of potential wells at short Ag−Ag distances. The data in this study suggest the significance of ligand-unsupported silver−silver interactions (argentophilicity) in $Tl[Ag(CN)_2]$. Tl−Ag interactions are determined to be insignificant in the compound. $Tl[Ag(CN)_2]$ crystallizes in the monoclinic space group $P2_1/c$ (No. 14), with $a = 7.798(1)$ Å, $b = 14.685(3)$ Å, $c = 8.566(2)$ Å, $\beta = 91.66(2)°$, $Z = 8$, $R = 0.0643$, and $R_w = 0.0899$.

Introduction

Coordination compounds of the d^{10} monovalent ions of group 11 have received tremendous attention in the last twenty five years. A central issue in the chemistry of these complexes is the study of closed-shell metal−metal interactions. Molecular and electronic structure studies of gold(I) complexes are under ongoing investigation by several research groups.[1−12] Recent work includes simple monomeric complexes[1−5] as well as dinuclear and polynuclear clusters of Au(I).[5−12] Similarly, coordination complexes of Cu(I) have been thoroughly investigated for their structural and spectral properties.[13−19] Most of these studies have been for tetranuclear clusters of the type $Cu_4X_4L_4$ (X = halogen; L = amine or phosphine) due to their rich luminescence properties. Surprisingly, silver is by far the least investigated coinage metal despite being in the same group as copper and gold. Very few spectroscopic investigations have been reported for Ag(I) molecular coordination compounds.[19−23]

A study of lanthanide ion complexes of $Ag(CN)_2^-$ and $Au(CN)_2^-$ has been carried out in our laboratory.[24] Also, we have recently reported the first example of $Ag(CN)_2^-$ lumines-

[†] University of Maine.
[‡] Auburn University.
[§] ORNL.
[||] Angelo State University.

(1) Larson, L. J.; McCauley, E. M.; Weissbart, B.; Tinti, D. S. *J. Phys. Chem.* **1995**, *99*, 7218.
(2) Striplin, D. R.; Crosby, G. A. *J. Phys. Chem.* **1995**, *99*, 11041.
(3) (a) Fischer, P.; Ludi, A.; Patterson, H. H.; Hewat, A. W. *Inorg. Chem.* **1994**, *33*, 62. (b) Nagle, J. K.; LaCasce, J. H., Jr.; Dolan, P. J., Jr.; Corson, M. R.; Assefa, Z.; Patterson, H. H. *Mol. Cryst. Liq. Cryst.* **1990**, *181*, 359. (c) Nagasundaram, N.; Roper, G.; Biscoe, J.; Chai, J. W.; Patterson, H. H.; Blom, N.; Ludi, A. *Inorg. Chem.* **1986**, *25*, 2947. (d) Patterson, H. H.; Roper, G.; Biscoe, J.; Ludi, A.; Blom, N. *J. Lumin.* **1984**, *31/32*, 555. (e) Markert, J. T.; Blom, N.; Roper, G.; Perregaux, A. D.; Nagasundaram, N.; Corson, M. R.; Ludi, A.; Nagle, J. K.; Patterson, H. H. *Chem. Phys. Lett.* **1985**, *118*, 258.
(4) (a) Koutek, M. E.; Mason; W. R. *Inorg. Chem.* **1980**, *19*, 648. (b) Mason, W. R. *J. Am. Chem. Soc.* **1976**, *98*, 5182. (c) Savas, M. M.; Mason; W. R. *Inorg. Chem.* **1987**, *26*, 301. (d) Jaw, H. R.; Savas, M. M.; Rogers, R. D.; Mason; W. R. *Inorg. Chem.* **1989**, *28*, 1028. (e) Chastain, S. K.; Mason, W. R. *Inorg. Chem.* **1982**, *21*, 3717.
(5) (a) McClesky, T. M.; Gray, H. B. *Inorg. Chem.* **1992**, *31*, 1733. (b) McClesky, T. M.; Mizoguchi, T. J.; Richards, J. H.; Gray, H. B. *Inorg. Chem.* **1996**, *35*, 3434.
(6) Pathaneni, S. S.; Desiraju, G. R. *J. Chem. Soc., Dalton Trans.* **1993**, 319.
(7) (a) Cerrada, E.; Jones, P. G.; Laguna, A.; Laguna, M. *Inorg. Chem.* **1996**, *35*, 2995. (b) Cerrada, E.; Laguna, A.; Laguna, M.; Jones, P. G. *J. Chem. Soc., Dalton Trans.* **1994**, 1325.
(8) (a) Assefa, Z.; McBurnett, B. G.; Staples, R. J.; Fackler, J. P., Jr.; Assmann, B.; Angermaier, K.; Schmidbaur, H. *Inorg. Chem.* **1995**, *34*, 75. (b) Forward, J. M.; Assefa, Z.; Staples, R. J.; Fackler, J. P., Jr. *Inorg. Chem.* **1996**, *35*, 16. (c) Assefa, Z.; Staples, R. J.; Fackler, J. P., Jr. *Inorg. Chem.* **1994**, *33*, 2790. (d) Fackler, J. P., Jr.; Staples, R. J.; Assefa, Z. *J. Chem. Soc., Chem. Commun.* **1994**, 431. (e) King, C.; Wang, J. C.; Khan, M. N. I.; Fackler, J. P., Jr.; *Inorg. Chem.* **1989**, *28*, 2145. (f) Khan, M. N. I., King, C.; Heinrich, D. D.; Fackler, J. P., Jr.; Porter, L. C. *Inorg. Chem.* **1989**, *28*, 2150. (g) Dávila, R., Elduque, A.; Grant, T.; Staples, R. J.; Fackler, J. P., Jr. *Inorg. Chem.* **1993**, *32*, 1749. (h) King, C.; Khan, M. N. I.; Staples, R. J.; Fackler, J. P., Jr. *Inorg. Chem.* **1992**, *31*, 3236.
(9) (a) Toronto, D. V.; Weissbart, B.; Tinti, D. S.; Balch, A. L. *Inorg. Chem.* **1996**, *35*, 2484. (b) Weissbart, B.; Toronto, D. V.; Balch, A. L.; Tinti, D. S. *Inorg. Chem.* **1996**, *35*, 2490. (c) Toronto, D. V.; Balch, A. L.; Tinti, D. S. *Inorg. Chem.* **1994**, *33*, 2507. (d) Balch, A. L.; Catalano, V. J.; Olmstead, M. M. *Inorg. Chem.* **1990**, *29*, 585. (e) Balch, A. L.; Fung, E. Y.; Olmstead, M. M. *Inorg. Chem.* **1990**, *29*, 3203.
(10) Jones, W. B.; Yuan, J.; Narayanaswamy, R.; Young, M. A.; Elder, R. C.; Bruce, A. E.; Bruce, M. R. M. *Inorg. Chem.* **1995**, *34*, 1996.
(11) (a) Li, D.; Hong, X.; Che, C. M.; Lo, W. C.; Peng, S. M. *J. Chem. Soc., Dalton Trans.* **1993**, 2929. (b) Li, D.; Che, C. M.; Peng, S. M.; Liu, S. T.; Zhou, Z. Y.; Mak, T. C. W. *J. Chem. Soc., Dalton Trans.* **1993**, 189. (c) Shieh, S. J.; Li, D.; Peng, S. M.; Che, C. M. *J. Chem. Soc., Dalton Trans.* **1993**, 195. (d) Lee, C. F.; Chin, K. F.; Peng, S. M.; Che, C. M. *J. Chem. Soc., Dalton Trans.* **1993**, 467. (e) Che, C. M.; Kwong, H. L.; Yam, V. W. W.; Cho, K. C. *J. Chem. Soc., Chem. Commun.* **1989**, 885.

S0020-1669(97)00694-0 CCC: $15.00
Published on Web 03/04/1998

cence in $Tl[Ag(CN)_2]$.[25] Electronic structure calculations based on the extended Hückel method suggest the importance of metal−metal interactions in the compound.[25] To study the relative importance of Ag−Ag versus Tl−Ag interactions, we report herein the crystal structure of $Tl[Ag(CN)_2]$. Raman spectra as a function of temperature as well as further electronic structure calculations are also presented and discussed in terms of their relation to the crystal structure. A comparison can be made with $Tl[Au(CN)_2]$ in which we reported earlier that both Tl−Au and Au−Au interactions are significant.[26a]

Experimental Section

$Tl[Ag(CN)_2]$ crystals were grown by mixing a 1:1 mole ratio of TlCN and AgCN followed by slow evaporation of the aqueous solution. TlCN was prepared by passing HCN gas into an ether solution of thallium ethoxide (Aldrich), while AgCN was prepared by adding aqueous $AgNO_3$ to an ammoniacal solution of KCN (Sigma).

The structure of $Tl[Ag(CN)_2]$ was determined with data collected on a Nicolet R3m/V diffractometer by employing Mo Kα radiation (λ = 0.710 73 Å). All computations were performed with SHELXTL-PLUS VMX, Release 4.11.[26b] A colorless blade-shaped crystal with dimensions 0.14 × 0.18 × 0.35 mm was mounted on a glass fiber with epoxy cement at room temperature. The unit cell constants were determined by centering 24 reflections in the 2θ range 14−29°. Intensity data of the compound were collected for 1744 unique reflections ($+h$, $+k$, $\pm l$) in the $4 < 2\theta < 50°$ range by using the θ scanning technique. Two reflections established as standards were checked routinely for deviations of positions and intensities after every 100 reflections. Systematic absences of $l = 2n + 1$ in the $00l$ and $h0l$ and $k = 2n + 1$ for $0k0$ zones uniquely identified the space group as $P2_1/c$ (No. 14). Thallium and silver atoms were located by direct methods. Carbon and nitrogen atoms were located from difference maps calculated after least-squares refinement of the heavy atom positions. The data were corrected for Lorentz and polarization effects and for absorption by empirical methods on azimuthal (ψ) scans of reflections. The structure was refined using full-matrix least-squares methods on F; anomalous scattering contributions were included. No extinction correction was performed. A final difference map showed significant electron density around the Tl atom. All the atoms were ultimately refined anisotropically.

Raman spectra were recorded with a holographic double monochromator (Ramanor 2000 M) equipped with a Pelletier cooled quantum photometer (model 1140, Princeton Applied Research). The 514.5 nm green line of an argon ion laser (Coherent, Innova 90-2A) was used as the light source. Raman spectra were recorded as a function of temperature between 10 K and room temperature. Liquid helium was used as the coolant in a model Lt-3-110 Heli-Tran cryogenic liquid transfer system equipped with a temperature controller. In all spectra single crystals of high optical quality were selected using a microscope. Care was taken in the Raman experiment to ensure that the crystal did not decompose. The laser power was adjusted between 3 and 20 mW depending on the Raman signal. Fourier transform infrared (FTIR) spectra were obtained using a Bio-Rad Digilab FTS-60 spectrometer equipped with a microscope accessory and a liquid nitrogen-cooled detector. This setup allows measurement of the infrared spectra for single crystals using the reflectance mode.

The computational method was of the extended Hückel type using FORTICON8 program (QCMP011). Relativistic parameters were used for all atoms, and the details are described elsewhere.[25] The atom separations were according to the crystal structure of $Tl[Ag(CN)_2]$ as discussed below. The Ag−Ag distance was varied, and the resulting total energy was determined in a trimer, $[Ag(CN)_2^-]_3$, and a pentamer, $[Ag(CN)_2^-]_5$, model which describe silver−silver interactions in $Tl[Ag(CN)_2]$. Approximations were made that all $Ag(CN)_2^-$ ions were linear in both models, the terminal ions are perpendicular to the central ion in the trimer (dihedral angle = 90°) and parallel in the pentamer (dihedral angle = 0°), and the pentamer has a square planar (undistorted) geometry. Therefore, the point group is D_{2h} for the trimer model and D_{4h} for the pentamer model.

Results

(1) Crystal Structure. Crystallographic data for the title compound are shown in Table 1. Atomic positional and thermal parameters are given in Table 2. Significant interatomic distances and bond angles are given in Table 3. The thermal ellipsoid drawing of the unit cell is shown in Figure 1. The structure displays a layered arrangement in which layers of Tl^+ ions alternate with silver layers along the a axis. The packing diagram in Figure 2 shows this arrangement.

There are three crystallographically inequivalent Ag sites in the unit cell. Two of these sites, Ag(1) and Ag(2), appear on inversion centers while the third one, Ag(3), lies on a general position. The $Ag(CN)_2^-$ ions are stacked in two patterns throughout the crystal structure of the title compound, one pattern in the environment of each Ag site on an inversion center, namely, Ag(1) and Ag(2). The stacking in the Ag(1) environment appears as a trimer of interacting $Ag(CN)_2^-$ ions with a linear arrangement for the three Ag atoms. The Ag(1) atom is surrounded by two opposite images of Ag(3) in this

(12) (a) Lange, P.; Schier, A.; Schmidbaur, H. *Inorg. Chem.* **1996**, *35*, 637. (b) Bachman, R. E.; Schmidbaur, H. *Inorg. Chem.* **1996**, *35*, 1399. (c) Sladek, A.; Schmidbaur, H. *Inorg. Chem.* **1996**, *35*, 3268. (d) Chung, S. C.; Krüger, S.; Schmidbaur, H. Rösch, N. *Inorg. Chem.* **1996**, *35*, 5387. (e) Lange, P.; Beruda, H.; Hiller, W.; Schmidbaur, H. *Z. Naturforsch.* **1994**, *49B*, 781. (f) Görling, A.; Rösch, N.; Ellis, D. E.; Schmidbaur, H. *Inorg. Chem.* **1991**, *30*, 3986. (g) Scherbaum, F.; Grohmann, A.; Huber, B.; Krüger, C.; Schmidbaur, H. *Angew Chem.* **1988**, *100*, 1602; *Angew. Chem., Int. Ed. Engl.* **1988**, *27*, 1544. (h) Scherbaum, F.; Grohmann, A.; Müller, G.; Schmidbaur, H. *Angew. Chem.* **1989**, *101*, 464; *Angew. Chem., Int. Ed. Engl.* **1989**, *28*, 463. (i) Grohmann, A.; Riede, J.; Schmidbaur, H. *Nature* **1990**, *345*, 140. (j) Schmidbaur, H. *Gold Bull.* **1990**, *23*, 11.

(13) (a) Simon, J. A.; Palke, W. E.; Ford, P. C. *Inorg. Chem.* **1996**, *35*, 6413. (b) Ford, P. C. *Coord. Chem. Rev.* **1994**, *132*, 129. (c) Tran, D.; Ryu, C. K.; Ford, P. C. *Inorg. Chem.* **1994**, *33*, 5957. (d) Kyle, K. R.; Ryu, C. K.; DiBenedetto, J. A.; Ford, P. C. *J. Am. Chem. Soc.* **1991**, *113*, 2954. (e) Ryu, C. K.; Kyle, K. R.; Ford, P. C. *Inorg. Chem.* **1991**, *30*, 3982. (f) Kyle, K. R.; DiBenedetto, J. A.; Ford, P. C. *J. Chem. Soc., Chem. Commun*, **1989**, 714. (g) Kyle, K. R.; Ford, P. C. *J. Am. Chem. Soc.* **1989**, *111*, 5005. (h) Kyle, K. R.; Palke, W. E.; Ford, P. C. *Coord. Chem. Rev.* **1990**, *97*, 35. (i) Døssing, A.; Kudo, S.; Ryu, C. K.; Ford, P. C. *J. Am. Chem. Soc.* **1993**, *115*, 5132. (j) Ryu, C. K.; Vitale, M.; Ford, P. C. *Inorg. Chem.* **1993**, *32*, 869. (k) Vitale, M.; Ryu, C. K.; Palke, W. E.; Ford, P. C. *Inorg. Chem.* **1994**, *33*, 561.

(14) (a) Hardt, H. D.; Stroll, H. J. *Z. Anorg. Allg. Chem.* **1981**, *480*, 193. (b) Hardt, H. D.; Stroll, H. J. *Z. Anorg. Allg. Chem.* **1981**, *480*, 199. (c) Hardt, H. D.; Pierre, A. *Inorg. Chim. Acta* **1977**, *25*, L59. (d) Hardt, H. D.; Pierre, A. *Annal. Univ. Sarav.* **1980**, *15*, 7.

(15) Eitel, E.; Oelkrug, D.; Hiller, W.; Strähle, J. *Z. Naturforsch.* **1980**, *35B*, 1247.

(16) Vogler, A.; Kunkely, H. *J. Am. Chem. Soc.* **1986**, *108*, 7211.

(17) (a) Everly, R. M.; McMillen, D. R. *J. Phys. Chem.* **1991**, *95*, 9071. (b) Everly, R. M.; Ziessel, R.; Suffert, J.; McMillen, D. R. *Inorg. Chem.* **1991**, *30*, 559. (c) Casadonte, D. J., Jr.; McMillen, D. R. *J. Am. Chem. Soc.* **1987**, *109*, 331. (d) Casadonte, D. J., Jr.; McMillen, D. R. *Inorg. Chem.* **1987**, *26*, 3950. (e) Stacy, E. M.; McMillen, D. R. *Inorg. Chem.* **1990**, *29*, 393.

(18) Henary, M.; Zink, J. I. *J. Am. Chem. Soc.* **1989**, *111*, 7407.

(19) Sabin, F.; Ryu, C. K.; Ford, P. C.; Vogler, A. *Inorg. Chem.* **1992**, *31*, 1941.

(20) Vogler, A.; Kunkely, H. *Chem. Phys. Lett.* **1989**, *158*, 74.

(21) Henary, M.; Zink, J. I. *Inorg. Chem.* **1991**, *30*, 3111.

(22) Ford, P. C.; Vogler, A. *Acc. Chem. Res.* **1993**, *26*, 220.

(23) Kutal; C. *Coord. Chem. Rev.* **1990**, *99*, 213.

(24) (a) Assefa, Z.; Shankle, G.; Patterson, H. H.; Reynolds, R. *Inorg. Chem.* **1994**, *33*, 2187. (b) Assefa, Z.; Patterson, H. H. *Inorg. Chem.* **1994**, *33*, 6194.

(25) Omary, M. A.; Patterson, H. H.; Shankle, G. *Mol. Cryst. Liq. Cryst.* **1996**, *284*, 399.

(26) (a) Assefa, Z.; DeStefano, F.; Garepapaghi, M. A.; LaCasce, J. H., Jr.; Ouellete, S.; Corson, M. R.; Nagle, J. K.; Patterson, H. H. *Inorg. Chem.* **1991**, *30*, 2868. (b) *SHELXTL-PLUS VMX*, Release 4.11; Siemens Analytical X-ray Instruments: Madison, WI, 1990.

Table 1. Crystallographical Data for $Tl[Ag(CN)_2]$

empirical formula	C_2AgN_2Tl
fw	364.3
cryst syst	monoclinic
space group	$P2_1/c$ (No. 14)
a, Å	7.798(1)
b, Å	14.685(3)
c, Å	8.566(2)
β, deg	91.66(2)
V, Å^3	980.5(3)
Z	8
d_{calcd}, g/cm^3	4.935
abs coeff, cm^{-1}	369.7
cryst size (mm)	0.1 × 0.18 × 0.35
no. of reflcns collctd	1964
no. of unique (merging R)	1744 (0.0548)
no. of obsd ($F_0 > 4\sigma F_0$)	1240
2θ range, deg	4.0−50
data:params	11:1
abs correction	semiempirical
transm factor: max, min	0.0284, 0.0113
largest peak and hole, e Å^{-3}	2.22 and 1.96
R,[a] R_w [b]	0.0643, 0.0899
goodness-of-fit	0.89

[a] $R = \sum||F_0| - |F_C||/\sum|F_0|$. [b] $R_w = [\sum w(|F_0| - |F_C|)^2/\sum w F_0 2]^{1/2}$ (*International Tables for X-ray Crystallography*; Kynoch Press: Birmingham, England, 1974; Vol. IV).

Table 2. Atomic Coordinates (×10^4) and Equivalent Isotropic Displacement Coefficients (Å^2 × 10^3)

	x	y	z	U(eq)[a]
Tl(1)	3026(2)	7610(1)	5268(1)	42(1)
Tl(2)	2263(2)	10480(1)	4689(2)	54(1)
Ag(1)	0	10000	0	56(1)
C(1)	−1120(38)	10683(20)	1814(34)	42(9)
N(1)	−1658(43)	11003(27)	2880(38)	79(13)
Ag(2)	5000	10000	0	64(1)
C(2)	4739(50)	9353(22)	2171(38)	57(13)
N(2)	4718(25)	9122(16)	3356(35)	44(8)
Ag(3)	−2029(3)	8201(2)	451(3)	53(1)
C(3)	−3528(34)	8168(17)	−1627(34)	37(8)
N(3)	−4128(35)	8212(18)	−2772(29)	50(9)
C(4)	−346(35)	8360(19)	2354(42)	49(11)
N(4)	549(37)	8544(21)	3445(39)	62(11)

[a] Equivalent isotropic U defined as one-third of the trace of the orthogonalized $\mathbf{U}_{ij}$ tensor.

Table 3. Selected Interatomic Distances (Å) and Angles (deg) for $Tl[Ag(CN)_2]$

Ag(1)−C(1)	2.06(3)	C(1)−Ag(1)−C(1A)	180
Ag(2)−C(2)	2.10(3)	Ag(1)−C(1)−N(1)	174.1(29)
Ag(3)−C(3)	2.10(3)	C(2)−Ag(2)−C(2A)	180
C(1)−N(1)	1.12(4)	Ag(2)−C(2)−N(2)	170.3(32)
C(2)−N(2)	1.07(4)	C(3)−Ag(3)−C(4)	172.3(11)
C(3)−N(3)	1.08(4)	Ag(3)−C(3)−N(3)	170.7(26)
Ag(1) −Ag(3)	3.110(3)	Ag(3)−C(4)−N(4)	172.9(26)
Ag(2)−Ag(3)	3.528(3)		
Ag(1)−Ag(2)	3.899(1)		
Tl(1)−N(2)	3.08(2)		
Tl(1)−N(1A)	2.81(4)		
Tl(1)−N4	2.81(3)		
Tl(2)−N(2)	3.01(2)		
Tl(2)−N(4)	3.30(3)		

environment (Figure 1) with an Ag(1)−Ag(3) contact of 3.110(3) Å. The $Ag(CN)_2^-$ ions are oriented in a nearly perpendicular geometry with a Ag(1)−Ag(3)−C(3) angle of 98°. The other stacking pattern is observed in the Ag(2) environment and can be described as a pentamer of $Ag(CN)_2^-$ ions with a distorted square planar geometry. Silver−silver contacts of 3.528(3) and 3.899(1) Å are present between the central Ag(2) atom with each of the opposite images of the Ag(3) and Ag(1)

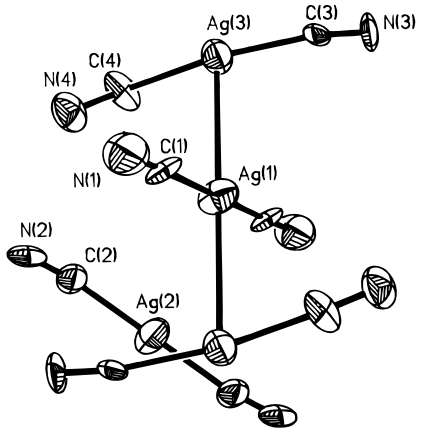

Figure 1. Thermal ellipsoid plot of $Tl[Ag(CN)_2]$ showing the three crystallographically distinct sites for the Ag atoms.

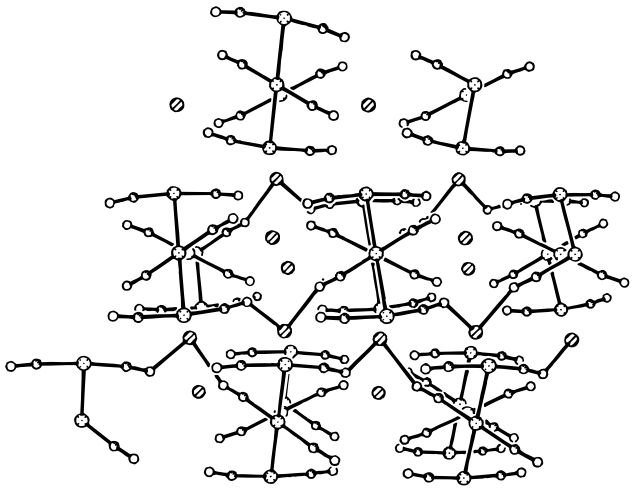

Figure 2. Packing diagram along the *a* axis showing the layered arrangements of the $Tl[Ag(CN)_2]$ structure. Notice that silver layers alternate with thallium layers.

terminal atoms, respectively. The $Ag(CN)_2^-$ ions of the Ag(1) and Ag(2) sites are required to be linear with a C−Ag−C angle of 180°. The coordination of the $Ag(CN)_2^-$ ion at the Ag(3) site slightly deviates from linearity; the C(3)−Ag(3)−C(4) angle is 172.3(1)°. The $Ag(CN)_2^-$ ions at the Ag(2) sites are oriented parallel to the *b* axis while the other two ions lie parallel to the *ab* plane.

The crystal structure of the compound indicates the presence of two crystallographically distinct Tl sites each of which is on a general position. Figure 3 shows the environments surrounding both Tl sites. The coordination around thallium is irregular, where four N atoms surround Tl(1) in a distorted square pyramidal arrangement with the Tl atom out of the plane. The Tl−N distance ranges between 2.81(3) and 3.07(2) Å in that site. Meanwhile, Tl(2) is surrounded by six neighboring N atoms in a distorted octahedral arrangement. The Tl−N contact at the Tl(2) site is longer than that observed at the Tl(1) site and ranges between 2.94 and 3.31 Å (Table 3). The shortest contact between the Tl and Ag atoms is about 4 Å.

(2) Vibrational Spectra. The high- and low-energy regions of the Raman spectra for $Tl[Ag(CN)_2]$ are shown in Figures 4 and 5, respectively, at 10 K, 80 K, and room-temperature. Assignments of the Raman bands are given in Table 4. The room-temperature Raman spectra are not well-resolved, but better resolution was obtained in the spectra recorded at 10 and 80 K. Infrared spectra at room temperature show two peaks in

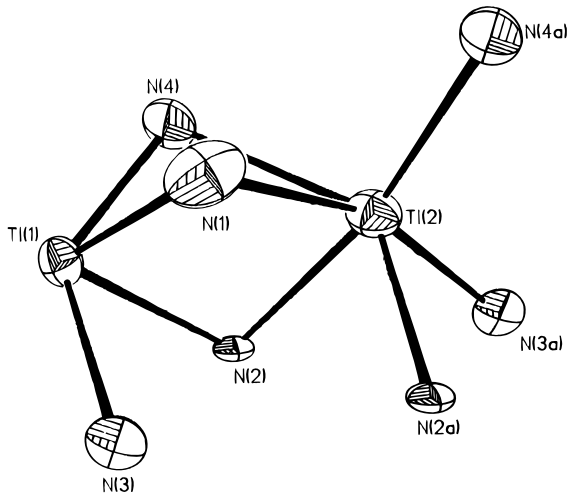

Figure 3. Environment of the two thallium sites in the crystal structure of Tl[Ag(CN)$_2$].

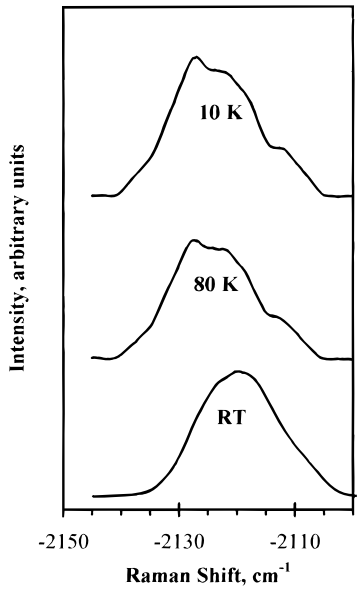

Figure 4. Raman spectrum of Tl[Ag(CN)$_2$] in the ν_{C-N} region recorded at 10 K (top), 80 K (middle), and room temperature (bottom).

the ν_{C-N} region at 2107 and 2115 cm^{-1}. Raman and infrared data for polycrystalline Tl[Ag(CN)$_2$] at room temperature were reported previously by Chadwick and Frankiss, but no spectra were shown.[27] Our room-temperature Raman and infrared data are similar to the data in that study.

(3) Electronic Structure Calculations. The trimer and pentamer arrangements of the Ag(CN)$_2^-$ ions according to the crystal structure have been modeled by extended Hückel calculations in order to gain better insight into the Ag−Ag bonding in Tl[Ag(CN)$_2$]. Figure 6 shows that a potential well forms at an Ag−Ag distance of 2.79 and 3.44 Å in the trimer and pentamer model, respectively. Table 5 summarizes the results of the calculations for the minimized structures of the two models.

Discussion

(1) Raman Data. Four peaks have been resolved within the strongest Raman bands at ca. 2120 and 250 cm^{-1} as shown in Figures 4 and 5, respectively. This result is in agreement with

(27) Chadwick, B. M.; Frankiss, S. G. *J. Mol. Struct.* **1968**, *2*, 281.

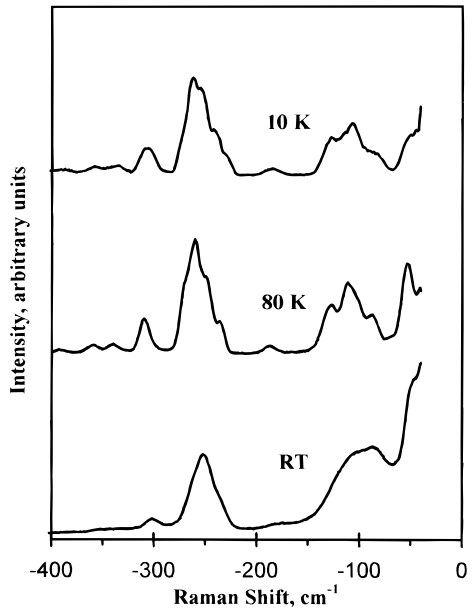

Figure 5. Raman spectrum of Tl[Ag(CN)$_2$] in the 0−400 cm^{-1} frequency range recorded at 10 K (top), 80 K (middle), and room temperature (bottom).

Table 4. Assignment of the Raman Bands for Tl[Ag(CN)$_2$]

cm^{-1}	assignment
<50	lattice bands
75−125	Ag−Ag stretch[a]
230−255	N−CAgC−N bend[b]
300−400	Ag−C stretch[b]
2110−2125	C−N stretch[b]

[a] There is overlap between the lattice bands and this band. However, the temperature dependence shown in Figure 5 suggests that this band is due to an Ag−Ag stretching mode. See text for further details. [b] This assignment is in agreement with the one reported by Chadwick and Frankiss.[27]

the crystal structure of Tl[Ag(CN)$_2$]. Although only three unique Ag atoms are present in the crystal structure, there are four unique cyanide groups. The cyanides on each of the two Ag atoms which appear on inversion centers, Ag(1) and Ag(2), are equivalent. In contrast, the Ag(3) atom lies on a general position, therefore giving rise to two structurally inequivalent cyanide groups in that position. Group-theoretical analysis was performed in order to calculate the number of ν_{C-N} peaks for Tl[Ag(CN)$_2$] according to the crystal structure. Since all Ag−Ag distances are relatively long in the Ag(2) environment, an isolated Ag(CN)$_2^-$ ion can be assumed at that site. Therefore, a $D_{\infty h}$ site symmetry is given for Ag(2). This gives rise to one Raman peak for ν_{C-N}. The much smaller Ag−Ag distance of 3.11 Å in the Ag(1) environment suggests that the site symmetry should be taken for the whole trimer arrangement of the three interacting Ag(CN)$_2^-$ ions in this environment. The point group is, consequently, D_{2h}. This gives rise to three Raman peaks in the ν_{C-N} region. Therefore, the total number of peaks according to this analysis is four, in agreement with the experimental data which shows ν_{C-N} peaks at 2137, 2127, 2123, 2113 cm^{-1} at low temperature. The large splitting of the two outer peaks (24 cm^{-1}) is too large for a correlation field effect and thus suggests the presence of [Ag(CN)$_2^-$] ions in more than one site,[27] in agreement with the crystal structure data.

The temperature dependence of the very low energy part of the Raman spectra provides more direct evidence for the significance of Ag−Ag interactions in Tl[Ag(CN)$_2$]. A careful inspection of Figure 5 reveals two different temperature-

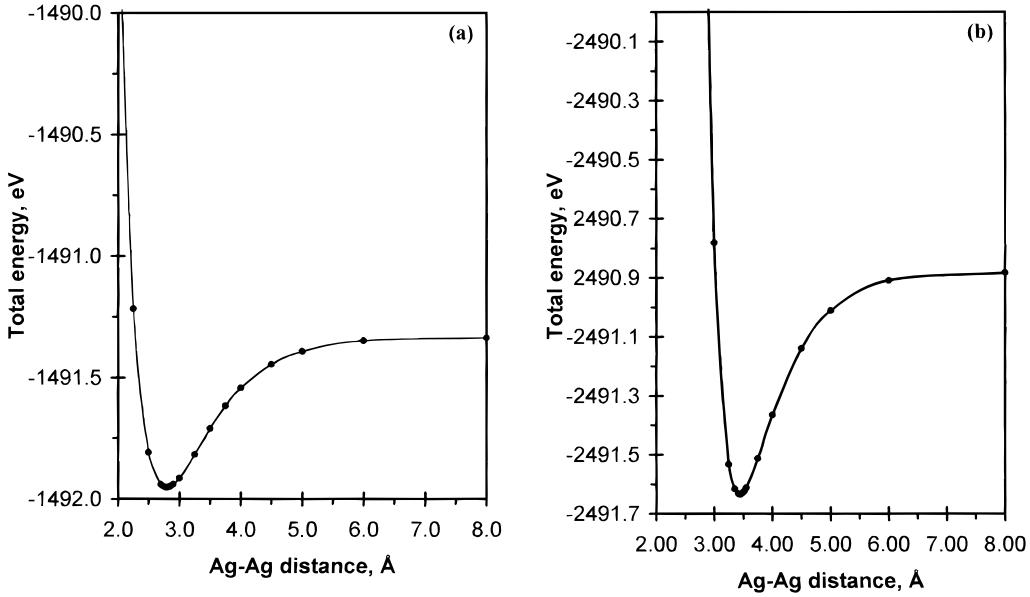

Figure 6. (a) Potential energy curve of the $[Ag(CN)_2^-]_3$ trimer model describing the Ag(1) environment in the crystal structure of $Tl[Ag(CN)_2]$ as obtained from relativistic extended Hückel calculations. The Ag−Ag distance is the distance between the central and the terminal silver atoms of the trimer. (b) Potential energy curve of the $[Ag(CN)_2^-]_5$ pentamer model describing the Ag(2) environment in the crystal structure of $Tl[Ag(CN)_2]$ as obtained from relativistic extended Hückel calculations. The Ag−Ag distance is the distance between the central and the terminal silver atoms of the pentamer.

Table 5. Summary of Extended Hückel Calculations for the Trimer and the Pentamer Models (Details of the Calculations Setup Are Given in the Text)

	model	
	trimer, $[Ag(CN)_2^-]_3$	pentamer, $[Ag(CN)_2^-]_5$
Ag−Ag equilibrium distance, Å	2.79	3.44
total energy, eV	−1491.95	−2491.63
energy per $[Ag(CN)_2^-]$ ion,[a] eV	−497.32	−498.33
binding energy,[b,c] eV	0.60	0.72
Ag−Ag overlap population[d]	0.034	−0.003
Ag−C overlap population[d]	0.237	0.244

[a] The corresponding values for the $[Ag(CN)_2^-]$ monomer and $[Ag(CN)_2^-]_2$ dimer are −497.13 and −497.19, respectively.[25] [b] The binding energy is calculated as the depth of the potential well relative to the energy at an Ag−Ag distance of 6.00 Å. [c] The corresponding value for the $[Ag(CN)_2^-]_2$ dimer is 0.13 eV.[25] [d] The overlap population values are given for bonds with the central Ag atom in both models. The Ag−C overlap population for an isolated $Ag(CN)_2^-$ ion is 0.258.

dependence patterns for two low-energy Raman bands. It is noted that the relative intensity of the broad band centered at ∼100 cm^{-1} increases relative to the band at ∼50 cm^{-1} as the temperature is cooled toward 10 K. It is expected that phonon or lattice bands become less important at lower temperatures. Therefore, we believe that the band at ∼100 cm^{-1} is not due to lattice vibrations but, instead, due to silver−silver bonding. In other words, the ∼100 cm^{-1} band is tentatively assigned to an Ag−Ag stretching mode (ν_{Ag-Ag}). It is noted that this band becomes more resolved at lower temperatures and three distinct peaks become apparent. More discussion of this Raman band will follow in the next section.

It is interesting to note that the ν_{C-N} frequencies observed in the Raman spectra of $Tl[Ag(CN)_2]$ are significantly lower than the corresponding frequencies for $K[Ag(CN)_2]$ and $Na[Ag(CN)_2]$ crystals reported elsewhere.[27,28] The room temperature ν_{C-N} band appears at ca. 2120 cm^{-1} in $Tl[Ag(CN)_2]$ which represents a shift of 26−30 cm^{-1} to lower frequency than the corresponding values in $K[Ag(CN)_2]$ and $Na[Ag(CN)_2]$. This is a large shift for salts of the same complex ion which differ only in the counter cation. A similar trend was noticed previously in the Raman data for $Tl[Au(CN)_2]$ versus other $M[Au(CN)_2]$ salts (M = K, Na, Li).[29] A possible explanation for the lower ν_{C-N} frequencies in the thallium compounds is the electron density of thallium surrounding the cyanide groups (Figure 3). The donation of the 6s electrons in Tl^+ to the empty antibonding orbitals of the cyanide ligands of appropriate symmetry (e.g., σ^*) should lower the ν_{C-N} value.

(2) Metal−Metal Interactions. The shortest Ag−Ag distance of 3.11 Å observed in $Tl[Ag(CN)_2]$ is shorter than any reported Ag−Ag distance among the silver dicyanide salts whose crystal structures have been determined. For example, the shortest silver−silver distance has been reported as 3.71 and 3.52 Å in $Na[Ag(CN)_2]$[30] and $K_2Na[Ag(CN)_2]_3$,[31] respectively. Crystal structures have also been determined for $K[Ag(CN)_2]$,[32] $M[Ag(CN)_2]_2{\cdot}2H_2O$ (M = Ca, Sr),[33] and $Rb\{Cd[Ag(CN)_2]_3\}$.[34] All of these compounds have Ag−Ag distances longer than 3.5 Å.

Table 5 suggests that the silver−silver interactions are greater in the trimer than in the pentamer because of the shorter Ag−Ag equilibrium distance and the greater Ag−Ag overlap population concomitant with a decreasing Ag−C overlap population for the trimer. In contrast, the pentamer arrangement gave rise to a greater Ag−Ag binding energy and a more negative total energy per $Ag(CN)_2^-$ unit than the trimer arrangement. Therefore the pentamer seems to have more

(28) (a) Wong, P. T. T. *J. Chem. Phys.* **1979**, *70*, 456. (b) Bottger, G. L. *Spectrochim. Acta* **1968**, *24A*, 1821. (c) Loehr, T. M.; Long, T. V., II. *J. Chem. Phys.* **1970**, *53*, 4182.
(29) (a) Chadwick, B. M.; Frankiss, S. G. *J. Mol. Struct.* **1976**, *31*, 1. (b) Stammreich, H.; Chadwick, B. M.; Frankiss, S. G. *J. Mol. Struct.* **1967/1968**, *1*, 191.
(30) Range, K. J.; Kühnel, S.; Zabel, M. *Acta Crystallogr.* **1989**, *C45*, 1419.
(31) Zabel, M.; Kühnel, S.; Range, K. J. *Acta Crystallogr.* **1989**, *C45*, 1619.
(32) (a) Hoard, J. L. *Z. Kristallogr.* **1933**, *84*, 231. (b) Staritzky, E. *Anal. Chem.* **1956**, *28*, 419.
(33) Range, K. J.; Zabel, M.; Meyer, H.; Fischer, H. *Z. Naturforsch.* **1985**, *40B*, 618.
(34) Hoskins, B. F.; Robson, R.; Scarlett, N. V. Y. *J. Chem. Soc., Chem. Commun.* **1994**, 2025.

Table 6. Charge Distribution in the Minimized Structures[a] for the Trimer and the Pentamer Models for Tl[Ag(CN)$_2$]

	central $Ag(CN)_2^-$ ion			terminal $Ag(CN)_2^-$ ions		
model	Ag	C	N	Ag	C	N
$[Ag(CN)_2^-]_3$	+0.65	−0.01	−0.78	+0.58	+0.013	−0.82
$[Ag(CN)_2^-]_5$	+0.60	−0.04	−0.76	+0.53	−0.025	−0.74

[a] The minimization was performed using extended Hückel calculations by varying the Ag−Ag distance in each model. The equilibrium distances are listed in Table 5.

thermodynamic stability. This discrepancy is partially due to the greater steric hindrance between the cyanide ligands in the pentamer (*N.B.*: the dihedral angle is 0° in the pentamer and 90° in the trimer).

The crystal structure of Tl[Ag(CN)$_2$] shows that the shortest Tl−Ag distance is about 4.0 Å indicating the absence of significant interaction between the two metals. This result is in contrast with our theoretical predictions. We have recently carried out extended Hückel calculations for an isolated Tl[Ag(CN)$_2$] molecule in which thallium is directly bonded to silver in a T-shaped (C_{2v}) arrangement.[25] A plot of the potential energy versus the Tl−Ag distance has resulted in the formation of a potential well at a Tl−Ag separation of 3.13 Å. These theoretical results predict the significance of Tl−Ag *metallophilic attraction*[35] in an isolated Tl[Ag(CN)$_2$] molecule. However, the crystal structure does not show isolated molecules of Tl[Ag(CN)$_2$] so this prediction does not hold. We attribute this discrepancy to the crystal field effects of the cyanide groups. The results of our extended Hückel calculations herein indicate that the negative charge is concentrated almost exclusively on the nitrogen atoms of the cyanide ligands in the minimized structure of both the trimer and the pentamer models described above. Table 6 summarizes the net charge distribution in both models. The highly negative charges on the nitrogen atoms are, therefore, predicted to attract the positive Tl^+ ions electrostatically in both models (Table 6). This prediction is confirmed by the crystal structure which shows that the thallium ions are surrounded by the nitrogen atoms of the cyanide ligand. There are two unique Tl^+ ions in the crystal structure of Tl[Ag(CN)$_2$] one of which is coordinated to four N atoms while the other has six nearest-neighbor N atoms (Figure 3). This Tl−N electrostatic attraction thus diminishes the expected weak Tl−Ag metallophilic attraction.

A similar situation to the Tl−N bonding in Tl[Ag(CN)$_2$] was found in $Tl_2[Pt(CN)_4]$. The crystal structure of $Tl_2[Pt(CN)_4]$ indicates that the two thallium atoms are surrounded by five neighboring nitrogen atoms of the cyanide ligands.[36] Density functional (DFT) calculations on that compound revealed that the bonding of Tl^+ to $[Pt(CN)_4]^{2-}$ has an ionic nature.[37] A recent theoretical study has been carried out for $Tl_2[Pt(CN)_4]$.[38] The calculated Tl−Pt separation was significantly shorter (287.7 pm) than the experimental value[36] of 314.0 pm, even at the Hartree−Fock level. Electron correlation effects were found to enhance the shortening of the Tl−Pt bond length. The authors attributed the longer experimental Tl−Pt distance to the crystal field effects of the cyanide ligands. These effects were found to overcompensate for the Tl−Pt metallophilic attraction and thus explain the relatively long Tl−Pt distance observed in the crystal structure.[38] It should be pointed out that the ligand field *f* factor for the cyanide group is 1.7 according to Jørgensen.[39] This value is among the highest for common ligands.

Our previous extended Hückel calculations for an isolated Tl[Ag(CN)$_2$] unit predict that the molecule has a net binding energy (depth of the potential well) of 0.26 eV at the calculated Tl−Ag equilibrium distance of 3.13 Å.[25] Similar calculations in the same study have been carried out for the $[Ag(CN)_2^-]_2$ dimer in which the two ions are parallel (D_{2h}). The silver dicyanide dimer has a total energy of −497.19 eV per $Ag(CN)_2^-$ ion at its equilibrium distance. This energy is only 0.06 eV more negative than the energy of an isolated $Ag(CN)_2^-$ ion according to these calculations.[25] Moreover, the equilibrium Ag−Ag distance in the minimized structure was 3.59 Å. These results actually suggest that the Tl^+ bonding to a monomeric $Ag(CN)_2^-$ ion should be stronger than the Ag−Ag bonding between two neighboring $Ag(CN)_2^-$ ions. Therefore, the metallophilic attraction is expected to be important for the Tl−Ag bonding as well as the Ag−Ag bonding in Tl[Ag(CN)$_2$]. However, as more $Ag(CN)_2^-$ ions come close to each other, the Ag−Ag interactions become more important. This is reflected in the decrease of the equilibrium Ag−Ag distance concomitant with a decreasing energy per $Ag(CN)_2^-$ ion as one proceeds from the monomer to the dimer[25] and then to either the trimer or the pentamer (Table 5). In the meantime, the aggregation of the $Ag(CN)_2^-$ units results in an increasing negative charge concentrated on the nitrogen atoms of the cyanide ligands while the positive charge is distributed between both silver and thallium atoms. In fact, Table 6 indicates that the total charge on silver atoms is only +1.81 on the three Ag atoms of the trimer and +2.71 in the pentamer. Meanwhile, the corresponding total charge on the N atoms are −4.84 and −7.42, respectively. The redundant negative charge has to be balanced by the Tl^+ ions. We conclude that the absence of significant Tl−Ag metallophilic attraction is due to a combined effect of increasing silver−silver interactions and increasing crystal field of the negatively charged cyanide ligands. These effects become more important with the increasing aggregation of the $Ag(CN)_2^-$ ions.

It is important to note that gold−gold interactions have been emphasized in several recent articles in the literature, and the term *aurophilic attraction* has been commonly used.[40] Silver−silver interactions, on the other hand, have received little attention due to the absence of enough experimental evidence for ligand-unsupported Ag−Ag interactions. Most examples reported to have short Ag−Ag separations were primarily dinuclear or polynuclear compounds of Ag(I) in which Ag−Ag interactions are assisted by the presence of bridging ligands.[41−45] Ligand-unsupported Ag−Ag interactions in the upper van der Waals limit have been suggested recently in the

(35) For a recent review of metallophilic attraction, see: Pyykkö, P. *Chem. Rev.* **1997**, *97*, 599.
(36) Nagle, J. K.; Balch, A. L.; Olmstead, M. M. *J. Am. Chem. Soc.* **1988**, *110*, 319.
(37) Ziegler, T.; Nagle, J. K.; Snijders, J. G.; Baerends, E. J. *J. Am. Chem. Soc.* **1989**, *111*, 5631.
(38) Dolg, M.; Pyykkö, P.; Runeberg, N. *Inorg. Chem.* **1996**, *35*, 7450.
(39) (a) Jørgensen, C. K. *Oxidation Numbers and Oxidation States*; Springer: New York, 1969; pp 84−85. (b) Jørgensen, C. K. *Absorption Spectra and Chemical Bonding in Complexes*; Pergamon Press: Oxford, 1962.
(40) For a review of aurophilic attraction, see: Schmidbaur, H. *Chem. Soc. Rev.* **1995**, 391.
(41) Papasergio, R. I.; Raston, C. L.; White, A. H. *J. Chem. Soc., Chem. Commun.* **1984**, 612.
(42) Gambarotta, S.; Floriani, C.; Chiesi-Villa, A.; Guastini, C. *J. Chem. Soc., Chem.* Commun. **1983**, 1087.
(43) Karsch, H. H.; Schubert, U. *Z. Naturforsch.* **1982**, *37B*, 186.
(44) Tsuda, T.; Ohba, S.; Takahashi, M.; Ito, M. *Acta Crystallogr.* **1989**, *C45*, 887.
(45) Kappenstein, C.; Ouali, A.; Guerin, M.; Cernák, J.; Chomic, J. *Inorg. Chim. Acta* **1988**, *147*, 189.

$[Ag_3(2\text{-}(3(5)\text{-}pz)py)_3]_2 \cdot 2py$ cluster.[46] Clusters of uncoordinated silver(I) ions have also been reported. An example is the octahedral Ag_6 cluster which has been detected in zeolites.[47] The importance of significant Ag−Ag interactions in the title compound lies in the fact that such interactions occur in a mononuclear coordination compound (not just Ag^+ ions) with no bridging ligands. The short Ag−Ag experimental distance of 3.11 Å observed in the Ag(1) environment is well below the 3.40 Å van der Waals' limit and close to the Ag−Ag distance in metallic silver (2.90 Å). To the best of our knowledge, $[Ag(imid)_2][ClO_4]$ (imid = imidazole) is the only other example reported for a coordination compound of Ag(I) with a shorter ligand-unassisted Ag−Ag distance than the title compound.[48] A silver−silver distance of 3.05 Å was reported in that example.

Besides the experimental evidence based on the short Ag−Ag distance in the crystal structure, the presence of significant Ag−Ag interactions in $Tl[Ag(CN)_2]$ is also supported theoretically. Our extended Hückel calculations indicate a thermodynamically favorable tendency of the $Ag(CN)_2^-$ units to aggregate. This is concluded from the decreasing total energy and increasing binding energy as one proceeds from the monomer to the dimer,[25] and then to the trimer and the pentamer (Table 5). The formation of potential wells for dimer,[25] trimer, and pentamer units of $Ag(CN)_2^-$ at relatively short Ag−Ag distances (Figure 6) provides further support for Ag−Ag bonding.

Since both the crystal structure and the theoretical calculations suggest that significant silver−silver interactions are present in $Tl[Ag(CN)_2]$, the tentative assignment of the Raman band at $\sim$100 cm^{-1} as due to Ag−Ag bonding gains additional strength. The position of the band (peak at $\sim$88 cm^{-1} at room temperature) is in the range where bands assigned to metal−metal stretching frequencies are observed.[49] A good comparison is with dimeric Ag(I) complexes of bridging phosphine ligands. Harvey et al. assigned Raman bands appearing at 76 cm^{-1} to Ag−Ag bonding in these compounds which have Ag−Ag distances in the 3.04−3.10 Å range.[50] Given the different geometry and the slight differences in the Ag−Ag distances between $Tl[Ag(CN)_2]$ and these dimeric compounds, the Raman data in the two cases are in good agreement.

Our results, hence, provide strong evidence for *argentophilicity* in $Tl[Ag(CN)_2]$ based on both experiment and theory. The fact that silver−silver interactions in $Tl[Ag(CN)_2]$ are ligand-unsupported suggests that argentophilicity is likely important in coordination compounds of Ag(I), in a similar way to *aurophilicity* in Au(I) compounds.

Conclusions

The significance of silver−silver interactions in $Tl[Ag(CN)_2]$ has been demonstrated both experimentally and theoretically in this study. The fact that these interactions occur in a mononuclear compound having nonbridging ligands provides strong evidence for the importance of ligand-unsupported argentophilicity in Ag(I) coordination compounds in general.

Acknowledgment. The authors thank Mr. David LaBreque for computerizing the Raman data acquisition. We also thank Dr. Thomas Schulze for his assistance with the Raman measurements. The valuable comments of Dr. Christian Reber on the manuscript are greatly appreciated. Z.A. acknowledges the support for a portion of his contribution from the Division of Chemical Sciences, Office of Basic Energy Sciences, U.S. DOE, DE-ACO5-R60R22464 with Lockhead Martin Energy Research Corporation.

Supporting Information Available: Tables of isotropic thermal parameters, complete listing of bond distances and bond angles, and full details of the data collection and stereodrawings (6 pages) are available. Ordering information is given on any current masthead page.

IC970694L

(46) Singh, K.; Long, J. R.; Stavropoulos, P. *J. Am. Chem. Soc.* **1997**, *119*, 2942.
(47) (a) Kim, Y.; Seff, K. *J. Am. Chem. Soc.* **1977**, *99*, 7055. (b) Kim, Y.; Seff, K. *J. Am. Chem. Soc.* **1978**, *100*, 175.
(48) Eastland, G. W.; Mazid, M. A.; Russell, D. R.; Symons, M. C. R. *J. Chem. Soc., Dalton Trans.* **1980**, 1682.
(49) For a review, see: Harvey, P. D. *Coord Chem. Rev.* **1996**, *153*, 175.
(50) Perreault, D.; Drouin, M.; Michel, A.; Miskowski, V. M.; Schaefer, W. P.; Harvey, P. D. *Inorg. Chem.* **1992**, *31*, 695.